



# Induction of tissue inhibitor of metalloproteinases-3 is a delayed early cellular response to hepatocyte growth factor

Paola Castagnino<sup>1</sup>, Jesus V Soriano<sup>2</sup>, Roberto Montesano<sup>2</sup> and Donald P Bottaro<sup>1</sup>

<sup>1</sup>Laboratory of Cellular and Molecular Biology, National Cancer Institute, National Institutes of Health, Bethesda, Maryland 20892, USA and <sup>2</sup>Department of Morphology, University Medical Center, Geneva, Switzerland

Hepatocyte growth factor (HGF) stimulates mitogenic, motogenic, and morphogenic responses in various cell types. We analysed HGF-responsive cells by differential display PCR to identify HGF-induced genes that mediate these biological events. One of the genes identified encoded a member of the tissue inhibitor of metalloproteinases (TIMP) family, TIMP-3. HGF transiently induced TIMP-3 mRNA in keratinocytes as well as kidney and mammary epithelial cells maximally between 4 and 6 h post-stimulation. Increased TIMP-3 protein secretion returned to basal levels within 18 h, while the expression of gelatinases A and B remained unchanged, suggesting that temporary suppression of matrix degradation is a delayed early response to HGF. Ectopic overexpression of TIMP-3 in cultured leiomyosarcoma cells conferred an epithelial morphology, reduced cell growth rate, anchorage-independent growth, and matrix invasion *in vitro*. Antisense suppression of TIMP-3 was associated with a scattered, fibroblastic cell morphology, as well as enhanced proliferation, anchorage-independent growth, and matrix invasion. A survey of tumor cell lines revealed an inverse relationship between metastatic potential and TIMP-3 expression level. These data suggest that early, transient TIMP-3 expression mediates specific HGF-induced phenotypic changes, and that loss of TIMP-3 expression may enhance the invasion potential of certain tumors.

**Keywords:** hepatocyte growth factor; TIMP-3; metalloproteinase; cell proliferation; gene induction

## Introduction

Hepatocyte growth factor (HGF) was originally identified as a potent mitogen for hepatocytes (reviewed in Michalopoulos and DeFrances, 1997) but also stimulates the proliferation of endothelial cells and a variety of epithelial cell types such as keratinocytes, melanocytes, and kidney epithelium (reviewed in Rubin *et al.*, 1993; Zarnegar and Michalopoulos, 1995). HGF also stimulates cell scattering (Stoker and Perryman, 1985), branching tubulogenesis (Montesano *et al.*, 1991), cellular invasion through extracellular matrix substrates (Giordano *et al.*, 1993; Rong *et al.*, 1994) and promotes tumor metastasis (Weidner *et al.*, 1990; Jeffers *et al.*, 1996). Multiple mRNA species tran-

scribed from a single HGF gene encode three distinct proteins: full-length HGF and two truncated HGF isoforms known as NK1 and NK2, which consist of the N-terminal domain linked in tandem with the first one or two kringle domains, respectively. Both truncated isoforms retain scatter activity, but their mitogenic activities differ substantially: while NK1 is mitogenically active with nearly the potency of HGF, NK2 displays little or no activity, and can potentially antagonize HGF-stimulated DNA synthesis (Chan *et al.*, 1991; Cioce *et al.*, 1996).

The biological responses of HGF are mediated by the c-Met proto-oncogene product (Bottaro *et al.*, 1991; Naldini *et al.*, 1991b; Weidner *et al.*, 1993), a transmembrane tyrosine kinase (Park *et al.*, 1987). Upon HGF binding, several tyrosine residues within the c-Met intracellular domain are phosphorylated, some of which are essential for catalytic activity (Naldini *et al.*, 1991a; Longati *et al.*, 1994), and some of which mediate the binding of signaling proteins such as Grb2 (Ponzetto *et al.*, 1994; Zhu *et al.*, 1994), the p85 subunit of phosphoinositide 3-kinase (PI3K; Ponzetto *et al.*, 1991; Graziani *et al.*, 1991; Bardelli *et al.*, 1992), phospholipase C- $\gamma$  (Bardelli *et al.*, 1992), Shc (Pellici *et al.*, 1995; Fixman *et al.*, 1995), and Gab1 (Weidner *et al.*, 1996). In Madin–Darby canine kidney (MDCK) epithelial cells, Grb2 binding is required for HGF-stimulated branching tubulogenesis (Fournier *et al.*, 1996), Gab1 is sufficient for tubulogenesis (Weidner *et al.*, 1996), and PI3K activity is required for both HGF-stimulated mitogenesis and scatter (Royal and Park, 1995; Rahimi *et al.*, 1996). The small GTP-binding proteins Rho and Rac are required for HGF-induced scatter and prior cytoskeletal rearrangements (Ridley *et al.*, 1995).

HGF-induced changes in gene expression include immediate increases in the expression of the transcription factors c-Fos and c-Jun, as well as c-Met (Boccaccio *et al.*, 1994). Later induction events correlate with HGF-induced epithelial and endothelial cell migration and morphogenesis, including increased production of transcription factor ETS1 (Fafeur *et al.*, 1997), urokinase-type plasminogen activator (u-PA), and its receptor (Pepper *et al.*, 1992), and the zinc finger protein slug (Savagner *et al.*, 1997). The HGF-stimulated proliferation and migration of keratinocytes that is thought to occur during wound healing (Matsumoto *et al.*, 1992; Gohda *et al.*, 1994; Watanabe *et al.*, 1994; Nusrat *et al.*, 1994; Sponsel *et al.*, 1994), is accompanied by the induction of collagenase (matrix metalloproteinase 1; MMP-1; Dunsmore *et al.*, 1996; Fafeur *et al.*, 1997) and stromelysin-1 (MMP-3; Dunsmore *et al.*, 1996). These induction events may be coordinated with the HGF-

stimulated induction of plasminogen activator inhibitor-1, resulting in appropriate spatial and temporal inhibition of matrix proteolysis (Pepper *et al.*, 1992; Wojta *et al.*, 1994).

We have surveyed HGF-responsive cell lines by differential display PCR (DD-PCR) to identify delayed early gene induction events that correlated with specific HGF biological activities. DD-PCR analysis of HGF-treated MDCK cells revealed the transient induction of tissue inhibitor of metalloproteinases-3 (TIMP-3). The specific biological impact of TIMP-3 expression was assessed by altering TIMP-3 levels in the absence of HGF treatment. Striking changes were observed in cell morphology, anchorage-independent cell growth, and cellular invasiveness *in vitro* that suggest a mechanism by which sustained HGF stimulation may promote cellular invasion and metastasis in certain human cancers.

## Results

### HGF-regulation of TIMP-3 transcription

Reverse transcribed mRNA from MDCK cells that had been stimulated with either HGF or HGF/NK2 for 6 h was subjected to DD-PCR. Differentially displayed bands were isolated from the gel, reamplified, and cloned. One of the clones encoded a member of the tissue inhibitor of metalloproteinases family (TIMP), TIMP-3. TIMP-3 mRNA level showed a dose-dependent increase in response to HGF treatment of MDCK cells (Figure 1a). HGF induction of TIMP-3 mRNA was observed at concentrations as low as 10 ng/ml of HGF, with maximal induction (tenfold) observed at 300 ng/ml. HGF/NK2 stimulated a lower level of TIMP-3 mRNA induction (approximately threefold) at much higher ligand concentrations (1000 ng/ml; Figure 1a). It is noteworthy that HGF/NK2 activates c-Met but does not stimulate DNA synthesis at any dose in any HGF target cell line tested (Chan *et al.*, 1991), suggesting

that the subset of c-Met signaling pathways activated by this HGF isoform are sufficient for TIMP-3 induction.

The temporal profile of TIMP-3 induction was examined by Northern analysis of RNA samples prepared from MDCK cells that had been treated with serum, HGF or HGF/NK2 for 1–20 h. TIMP-3 showed a dramatic increase in mRNA levels in response to HGF, with high levels of TIMP-3 mRNA being observed from 2–10 h (Figure 1b). Peak induction of TIMP-3 was observed after 4–6 h of growth factor exposure. Interestingly, a significant decrease in TIMP-3 message was observed after 10 h; at 20 h, HGF-stimulated cells displayed lower levels than untreated controls, suggesting that TIMP-3 production is tightly regulated by HGF. This is consistent with previous reports documenting the transient nature of serum-stimulated TIMP-3 induction in fibroblasts, where a striking correlation was found between TIMP-3 induction and the G1 phase of the cell cycle (Wick *et al.*, 1994). TIMP-3 induction by HGF/NK2 was similar in temporal profile to that of HGF, but decreased below control levels after 8 h of HGF treatment (Figure 1b).

The growth factor specificity of TIMP-3 induction was assessed by comparing the effects of several other growth factors, including epidermal growth factor (EGF), insulin-like growth factor-1 (IGF-1), platelet-derived growth factor (PDGF), keratinocyte growth factor (KGF), basic fibroblast growth factor (bFGF), transforming growth factor- $\beta$ 1 (TGF- $\beta$ ) and serum on TIMP-3 expression in MDCK cells. Northern analysis revealed that HGF and TGF- $\beta$  stimulated TIMP-3 mRNA induction fourfold and tenfold, respectively (Figure 2a). It is noteworthy that while TGF- $\beta$  can potentially suppress HGF-stimulated DNA synthesis in several epithelial cell types, it does not inhibit HGF-stimulated MDCK cell scattering (unpublished observations), and a recent report indicates that TGF- $\beta$  selectively inhibits HGF-stimulated branching morphogenesis in MDCK without blocking tubulogenesis (Sakurai and Nigam, 1997). Together these results

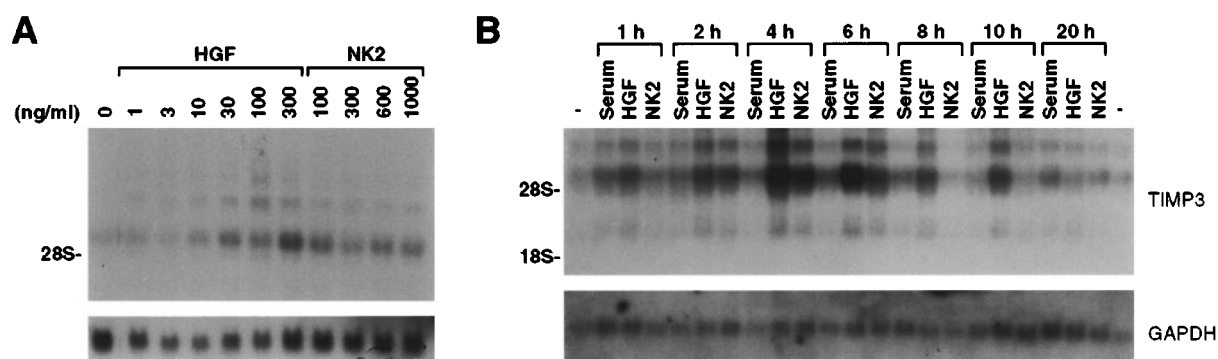


**Figure 1** (a) Northern analysis of the induction of TIMP-3 mRNA by HGF and HGF/NK2 in MDCK cells. Total RNA (15  $\mu$ g/sample) was isolated from MDCK cells that had been stimulated with the indicated concentrations (ng/ml) of HGF or HGF/NK2 for 6 h. The filter was first hybridized with a TIMP-3 cDNA probe (upper panel) and subsequently hybridized to a cDNA encoding glyceraldehyde 3-phosphate dehydrogenase (GAPDH, lower panel) to detect variations in sample loading. The location of the 28S ribosomal RNA on the TIMP-3 blot is shown on the left. (b) Northern analysis of the time course of TIMP-3 mRNA induction by HGF and HGF/NK2 in MDCK cells. Total RNA (15  $\mu$ g/sample) was prepared from MDCK cells treated with 5% fetal calf serum, HGF (50 ng/ml) or HGF/NK2 (300 ng/ml) for the indicated times. Filters were first hybridized with TIMP-3 cDNA (upper panel) and then GAPDH (lower panel). The position of the 28S and 18S ribosomal RNAs are marked on the left. The first and last lanes (–) of the blot contain total RNA prepared from serum-starved MDCK cells

suggest the convergence of HGF and TGF- $\beta$  intracellular signaling pathways at one or more levels.

TIMP-3 protein level was examined by immunoblot analysis of cell lysates prepared from serum-, TGF- $\beta$ , HGF/NK2- and HGF-stimulated MDCK cells. As shown in Figure 2b, TGF- $\beta$ , HGF/NK2 or HGF treatment stimulated significant increases in TIMP-3 protein relative to serum-treated controls. When MDCK cells were stimulated with TGF- $\beta$  and HGF together, no additive effects on TIMP-3 secretion were observed (data not shown). Interestingly, although TGF- $\beta$ , HGF/NK2 and HGF showed different levels of induction of TIMP-3 mRNA, each stimulated

TIMP-3 protein secretion to the same extent, suggesting that TIMP-3 expression may be regulated at both transcriptional and post-transcriptional levels. Together these data demonstrate that HGF and TGF- $\beta$  induce TIMP-3 gene transcription and stimulate increased TIMP-3 protein secretion in MDCK cells within the same time period.

To determine if other HGF-target cells also displayed the TIMP-3 response, two other epithelial cell lines, Balb/MK keratinocytes and B5/589 mammary epithelial cells (Rubin *et al.*, 1991) were analysed for TIMP-3 mRNA. As shown in Figure 2c, both cell lines were positive in this regard, suggesting that TIMP-3 induction may be part of a general response to HGF stimulation. HGF did not induce TIMP-3 in NIH3T3 fibroblasts, which do not express c-Met, but serum-stimulated induction of TIMP-3 was observed in these cells, and in B5/589 cells (Figure 2c).

#### Changes in the balance of TIMP-3 and gelatinase activities

The HGF-stimulated secretion of TIMP-3 is one means by which this growth factor may initiate extracellular matrix remodeling as observed in tissue culture model systems. The composition and rate of turnover of extracellular matrix is determined by a balance between the rates of synthesis and degradation of its components. Degradation is determined by a balance between the opposing activities of proteases and protease inhibitors. HGF-stimulated production of u-PA, MMP-1, and MMP-3 led to their gradual accumulation over 24–48 h (Pepper *et al.*, 1992; Dunsmore *et al.*, 1996), suggesting that during the period over which HGF transiently stimulates TIMP-3 production, the net protease/inhibitor balance may favor decreased matrix degradation. To test this hypothesis, we examined MMP levels over 18 h following HGF stimulation. TIMP-3 shows highest specific activity toward MMP-2 and -9 *in vitro* (Apte *et al.*, 1995), thus we focused on the production of these enzymes by two HGF-responsive cell lines. By SDS-PAGE/gelatin zymography, the majority of gelatinase activity present in MDCK cells appeared to be the 92 kDa MMP-9; very little 72 kDa MMP-2 was observed (Figure 3a). In contrast, the human leiomyosarcoma cell line SK-LMS-1 displayed prominent MMP-2 activity, and little detectable MMP-9 activity (Figure 3a). Although a detectable, transient increase in MMP-2 activity was observed in both cell lines at 4–6 h, no substantial changes were observed in the MMP-2 or MMP-9 activities in either cell line over 18 h (Figure 3a).

The MMP-2 and MMP-9 protein content of control or HGF-treated MDCK and SK-LMS-1 cells was examined specifically by immunoblotting of gelatin-Sepharose-fractionated conditioned medium (Figure 3b). Both MMP-2 and -9 bind tightly to this affinity matrix (Mazzei *et al.*, 1997). The 72 kDa MMP-2 was clearly detected in SK-LMS-1 cells, and although a subtle increase was detected at 4–6 h, no significant increase in the amount of MMP-2 was observed over this 18 h period. Little, if any 72 kDa MMP-2 was detected in medium conditioned by MDCK cells, consistent with the results observed by gelatin zymography (Figure 3a and b). Proteins with both

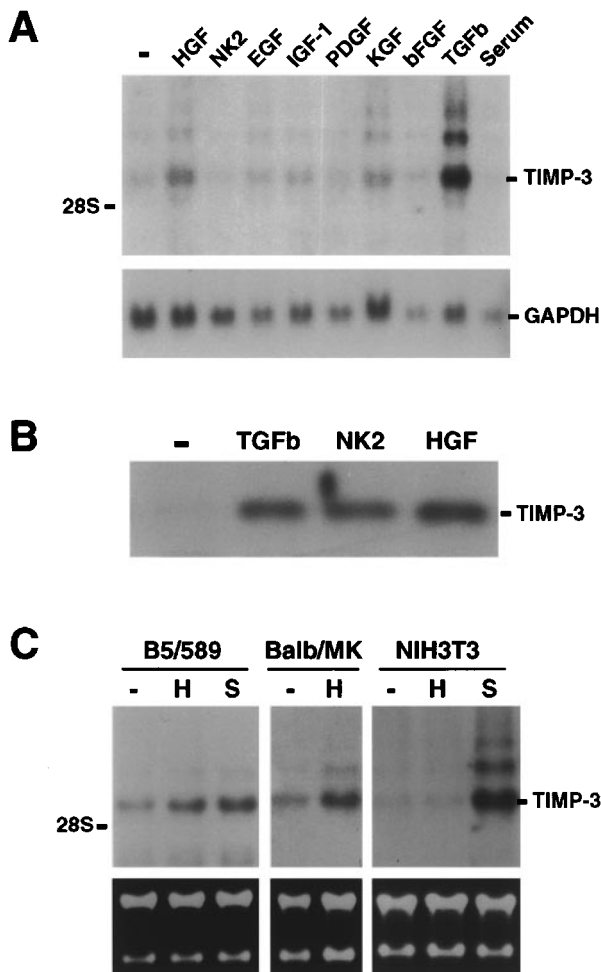


**Figure 2** (a) Northern analysis of TIMP-3 mRNA induction by various growth factors. Total RNA (15  $\mu$ g/sample) prepared from MDCK cells treated with the growth factors indicated (10 ng/ml) for 6 h was hybridized with either TIMP-3 (upper panel) or GAPDH (lower panel) probes. The first lane on the left (–) contains total RNA isolated from serum-starved MDCK cells. (b) Western blot analysis of TIMP-3 protein secretion by MDCK cells stimulated by HGF, HGF/NK2 or TGF- $\beta$ . Subconfluent MDCK cells were treated with serum (–), TGF- $\beta$  (10 ng/ml), HGF/NK2 (300 ng/ml) or HGF (100 ng/ml) for 6 h. Cell lysates (50  $\mu$ g/sample) were resolved by 14% SDS-PAGE, transferred to polyvinylidene difluoride (PVDF) membrane, and immunode- tected using anti-TIMP-3 antisera and chemiluminescence. (c) Northern analysis of TIMP-3 in B5/589 human mammary epithelial cells, Balb/MK keratinocytes, and NIH3T3 fibroblasts. Serum starved (–) cells were treated for 6 h with 50 ng/ml HGF (‘H’) or 10% serum (‘S’), as indicated above each lane, and RNA samples were prepared as described in Figure 1. Ethidium bromide staining of agarose gels is shown in the lower panels to verify equal sample loading

lower and higher molecular masses increased over the period, but these bands lacked gelatinase activity (Figure 3a and b). Although their identities are unknown, they were not observed when the same samples were probed with anti-MMP-9 and visualized using the same secondary antibody and detection system (Figure 3b, left and centre panels). Immunoblotting with anti-MMP-9 confirmed the identity of the 92 kDa gelatinase observed in MDCK cell conditioned medium, and showed that no significant increase in the production of this protein was evident after 6 h of HGF treatment (Figure 3b). No MMP-9 was detected in SK-LMS-1 cell conditioned medium (Figure 3b). Immunoblotting of MDCK cell extracts with anti-TIMP-3 under the same conditions clearly demonstrates the transient HGF-stimulated increase in TIMP-3 protein, peaking at 6 h (Figure 3b). Thus, production of these TIMP-3 sensitive proteases remained constant over the period of HGF-stimulated TIMP-3 induction, suggesting a transient shift in the protease/inhibitor balance toward protease inhibition.

#### HGF-independent modulation of TIMP-3 expression

We anticipated that the specific impact of TIMP-3 induction would be difficult to evaluate at the cellular level in light of the pleiotropic effects of HGF. To create a system in which TIMP-3 levels were modulated in the absence of other HGF-stimulated changes, we sought to identify a cell line with relatively low levels of TIMP-3 expression that would allow assessment of ectopic overexpression of TIMP-3, as

well as effective antisense suppression. A comparison of TIMP-3 expression by MDCK, SK-LMS-1, and NIH3T3 cells is shown in Figure 4. MDCK cells express 50-fold more TIMP-3 protein than any of the other cell lines under normal culture conditions. Thus, although several HGF activities have been well characterized using MDCK cells, they were not an optimal system for independently manipulating TIMP-3 expression. SK-LMS-1 cells displayed relatively low basal expression of TIMP-3, while NIH3T3 cells displayed an intermediate level (Figure 4). SK-LMS-1 cells were stably transfected with full-length sense and antisense TIMP-3 cDNA constructs, and antibiotic-resistant cultures were analysed for steady-state TIMP-3 protein expression level by immunoblotting. As shown in the right panel of Figure 4, the sense TIMP-3 transfectant displayed substantially increased TIMP-3 expression relative to control cells transfected with vector alone, while TIMP-3 expression was undetectable in the TIMP-3 antisense transfectants. The SK-LMS-1/TIMP-3 transfectants were thus ideally suited for evaluating the impact of TIMP-3 expression in the absence of other HGF-stimulated phenotypic changes.

#### TIMP-3-mediated changes in cell shape, growth and invasiveness

Striking morphological differences among the three SK-LMS-1 transfectants were immediately obvious (Figure 5). While the control vector transfectant resembled untransfected SK-LMS-1 cells (Figure 5, top panel), TIMP-3 overexpressing cells clustered into

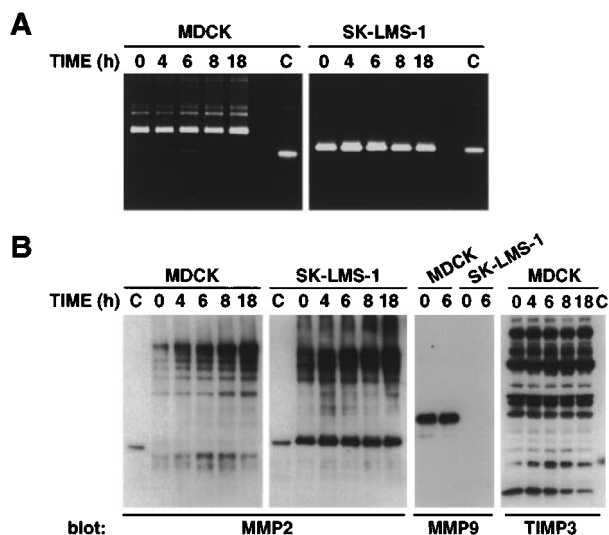


**Figure 3** (a) Gelatin zymography of control and HGF-treated MDCK and SK-LMS-1 cell conditioned medium. Subconfluent MDCK or SK-LMS-1 cells were treated with HGF (100 ng/ml) for the time intervals indicated above each lane. Conditioned medium was harvested, fractionated by gelatin-agarose affinity chromatography, and eluate was loaded onto SDS-PAGE/gelatin zymography gels. The lanes marked 'C' contain purified 72 kDa MMP-2. (b) Western blot analysis of MMP-2, MMP-9, and TIMP-3 protein production by MDCK and SK-LMS-1 cells stimulated by HGF. The level of MMP-2 and MMP-9 in the gelatin-sepharose eluates was verified by immunoblot analysis of equal volumes of conditioned media samples with anti-MMP-2 (left panels), or anti-MMP-9 (center panel). Induction of TIMP-3 in MDCK cells extracts was determined by immunoblot analysis (right panel). The lanes marked 'C' contain purified standards: 72 kDa MMP-2 (left panel), or TIMP-3 (right panel)

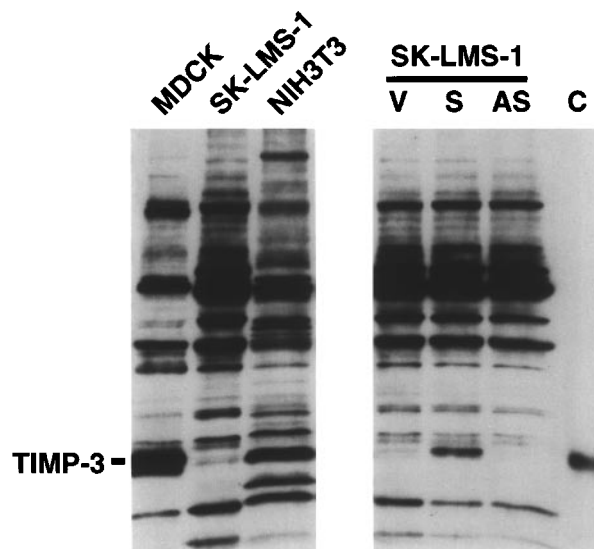


**Figure 4** Western blot analysis of TIMP-3 protein in MDCK, SK-LMS-1, NIH3T3 cells, and SK-LMS-1/TIMP-3 transfectants. Whole cell lysates were prepared from cells under normal growth conditions, and analysed by immunoblotting with anti-TIMP-3 antibody as described in Figure 2b. Note that in the left-hand panel, 80 µg of protein was loaded for each cell line except MDCK, where only 20 µg was loaded. Samples from stable SK-LMS-1 transfectants (right panel; 40 µg/sample) expressing vector (V), full-length TIMP-3 sense (S), or antisense (AS) constructs, were prepared similarly. The lane marked 'C' shows the migration of a purified TIMP-3 standard, the position of which is also indicated at the left

close-knit colonies, and generally had a more epithelial than fibroblastic appearance (Figure 5, centre panel). In contrast, TIMP-3 antisense transfectants grew as a uniform dispersion of randomly oriented single cells, each with elongated bipolar shape or occasionally with three or more thin cytoplasmic projections (Figure 5, bottom panel).

In addition to the gross morphological changes associated with the modulation of TIMP-3 expression,

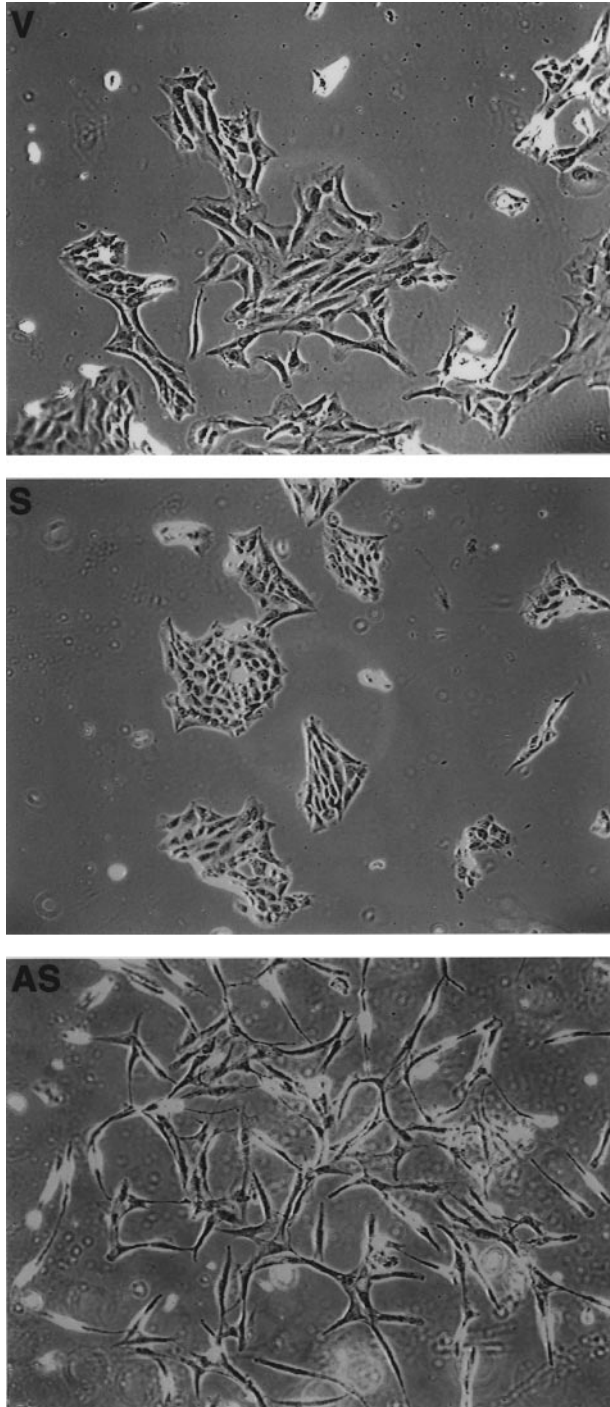


**Figure 5** Effects of TIMP-3 overexpression and antisense suppression on SK-LMS-1 cell morphology. Subconfluent SK-LMS-1 cells transfected with vector alone (V; top panel), full-length TIMP-3 cDNA (S; center panel), or full-length antisense TIMP-3 cDNA (AS; bottom panel) were photographed under normal growth conditions using phase contrast microscopy (10× objective magnification)

differences in the rate of growth of the transfectants were readily apparent. A comparison of the growth of sparsely-plated TIMP-3 transfectants over a period of 15 days is shown in Figure 6a. The growth of TIMP-3 overexpressors was obviously retarded relative to the control vector transfectant (Figure 6a, left and centre panels). We also observed accelerated growth of cells transfected with antisense to TIMP-3 (Figure 6a, right panel). The apparently dense staining of TIMP-3 overexpressors was due to dye precipitated onto the surface of these cells, and not to more dense packing of equal numbers of cells. To document these differences in more detail, the growth of the three SK-LMS-1/TIMP-3 transfectants was compared over a 20 day period (Figure 6b). The results confirmed the significantly faster growth of TIMP-3 antisense transfectants relative to TIMP-3 overexpressors ( $P < 0.001$  after 10 days; Figure 6b), and indicate that

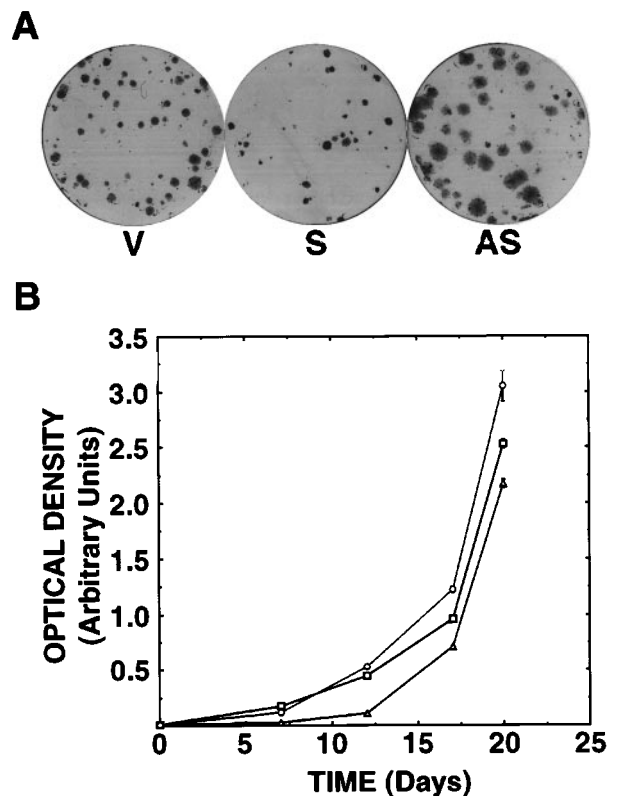


**Figure 6** (a) Effects of TIMP-3 overexpression and antisense suppression on SK-LMS-1 cell growth. Tissue culture dishes (6 cm) were seeded with SK-LMS-1 cells transfected with vector alone (V; left panel), full-length TIMP-3 cDNA (S; center panel), or full-length antisense TIMP-3 cDNA (AS; right panel) at a density of 100 cells/plate. After 15 days, the cells were fixed, stained with Giemsa, and photographed without magnification. (b) Time course of the effects of TIMP-3 on SK-LMS-1 cell growth. Multiwell tissue culture plates (6 cm) were seeded with SK-LMS-1 cells transfected with vector alone (open squares), full-length TIMP-3 cDNA (open triangles), or full-length antisense TIMP-3 cDNA (open circles) at a density of 100 cells/well. At times indicated on the X-axis, cells were fixed, stained with Giemsa, and cell proliferation in multiple wells was quantitated by scanning densitometry as described in Materials and methods. Mean values of optical density, in arbitrary units, are plotted on the Y-axis; error bars indicate standard error of the mean, and are smaller than the symbol size where not visible. Significant differences in growth ( $P < 0.001$ ) were observed between TIMP-3 sense and antisense transfectants at 10 days and thereafter

TIMP-3 can act as a growth suppressor under appropriate conditions.

Additional evidence supporting this hypothesis was found by evaluating the anchorage-independent growth of the three SK-LMS-1 transfectants in soft agar. Control vector transfectants exhibited a high level of colony formation in soft agar, consistent with their ability to form tumors in nude mice (Jeffers *et al.*, 1996). This level of colony formation was significantly decreased in TIMP-3 overexpressors (Figure 7, top and centre panels). In contrast, antisense suppression of TIMP-3 expression was associated with very aggressive colony formation in this assay, reaching a level eightfold greater than TIMP-3 overexpression (Figure 7, bottom panel). These results are consistent with those of Bian *et al* (1996), which show that TIMP-3 can act as a potent growth suppressor and that TIMP-3 can suppress the invasive phenotype that correlates

with aggressive growth in soft agar and tumorigenesis in nude mice.

We have examined several tumor cell lines to determine whether a correlation could be found between metastatic phenotype and TIMP-3 expression level. CaSki and HA1780 cells, derived from metastatic cervical and ovarian carcinomas, respectively, showed very low levels of TIMP-3, as did A204, a highly invasive rhabdomyosarcoma-derived cell line (Figure 8). HT1080 cells, derived from a fibrosarcoma, have been characterized as fourfold more invasive than normal fibroblasts, and threefold less invasive than A204 cells (Albini *et al.*, 1987). Interestingly, HT1080 cells express TIMP-3 at levels intermediate between M426 normal human fibroblasts, and A204 cells (Figure 8). RD, a rhabdomyosarcoma-derived cell line, grow as spindle shaped cells similar to the SK-LMS-1/TIMP-3 antisense transfectants, grow similarly in soft agar, and express similar levels of TIMP-3 protein (Figure 8 and data not shown). SAOS-2 cells are derived from an osteogenic sarcoma, display an epithelial-like morphology, but express much lower levels of TIMP-3 protein than the normal epithelial cells (B5/589 and MDCK) and fibroblasts (M426) included for comparison (Figure 8). Though preliminary, these data suggest that TIMP-3 expression correlates inversely with the invasive properties of certain human cancers.

The invasive properties of the SK-LMS-1/TIMP-3 transfectants were examined directly using three dimensional matrices of Matrigel or collagen I, both of which have been used extensively in the past to characterize the invasive properties of cultured cells. Cells were seeded on top of Matrigel matrices in growth medium alone or supplemented with HGF, and

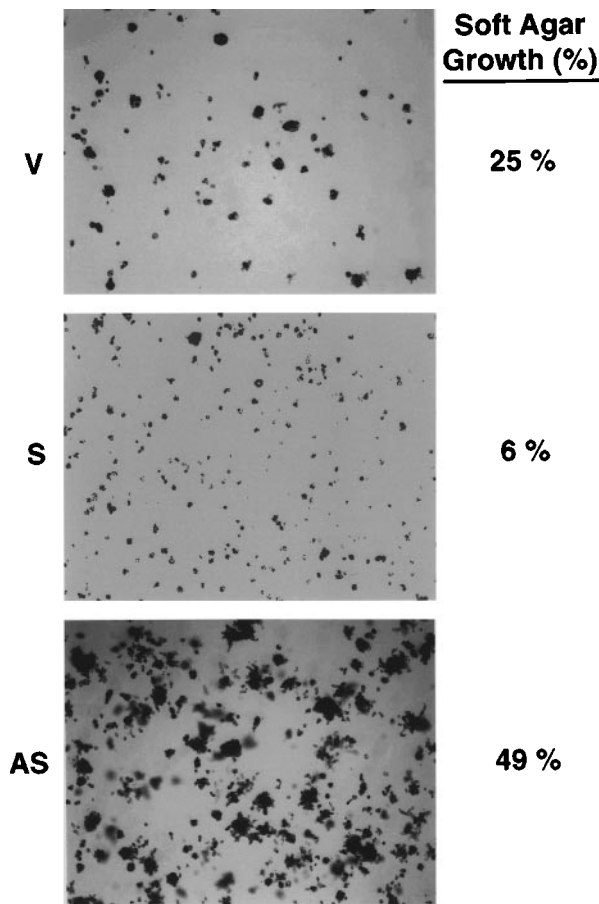


**Figure 7** Effects of TIMP-3 overexpression and antisense suppression on SK-LMS-1 cell anchorage-independent growth. SK-LMS-1 transfectants were plated at tenfold serial dilutions into soft agar as described in Materials and methods, allowed to grow for 15 days, then fixed and stained *in situ*. Brightfield photomicrographs of colonies formed by cells transfected with vector alone (V; top panel), full-length TIMP-3 cDNA (S; center panel), or full-length antisense TIMP-3 cDNA (AS; bottom panel) were taken using a  $2.5\times$  objective. A representative field of soft agar growth for each transfectant plated at  $1\times 10^5$  cells/plate is shown. Percentage of soft agar growth was determined by counting the number of cells forming colonies of diameter greater than  $50\ \mu\text{m}$  per total colony number. The percentage presented is the average of three measurements. Note in antisense transfectants many cell colonies of diameter greater than  $100\ \mu\text{m}$  were visualized

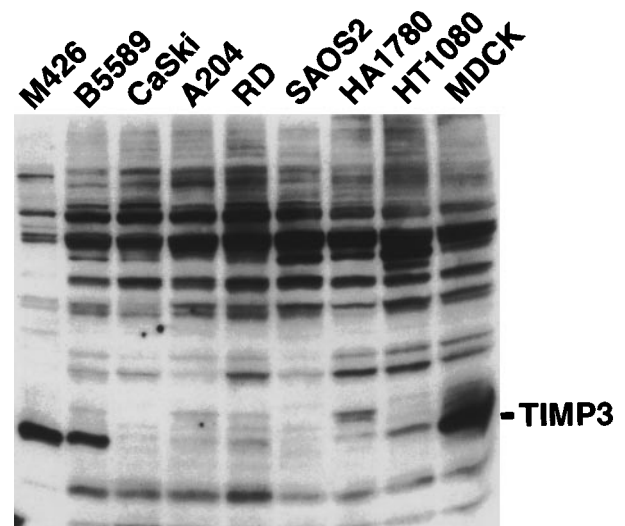


**Figure 8** Western blot analysis of increased TIMP-3 protein expression by normal and tumor cell lines. Cell lysates ( $50\ \mu\text{g}$ ) prepared from M426 embryonic lung fibroblasts, B5/589 mammary epithelial cells, CaSki epidermoid cervical carcinoma cells, A204 rhabdomyosarcoma cells, RD rhabdomyosarcoma cells, SAOS-2 osteogenic sarcoma cells, HA1780 ovarian carcinoma cells, HT1080 fibrosarcoma cells, and MDCK kidney epithelial cells ( $10\ \mu\text{g}$ ) were resolved by 12% SDS-PAGE, transferred to PVDF, and immunodetected using anti-TIMP-3 antisera and chemiluminescence. The position of the 24 kDa TIMP-3 protein band is indicated at the right



invasion was monitored daily by microscopy. After 3 days, control (vector-transfected) SK-LMS-1 cells displayed modest invasion into the underlying matrix (Figure 9, upper left panel), while the TIMP-3 antisense transfectants showed much more aggressive matrix invasion (Figure 9, upper right panel). In contrast, TIMP-3 overexpressors formed smooth-surfaced spheroid aggregates, and matrix invasion was completely abolished (Figure 9, upper centre panel). Stimulation with HGF moderately increased Matrigel invasion by control (vector) and antisense TIMP-3 transfectants, while in the TIMP-3 overexpressors an increase in the size of the spherical aggregates was observed, again in the total absence of Matrigel invasion (Figure 9, lower panels). Consistent with these findings were the invasive properties of the SK-LMS-1 transfectants observed using three-dimensional collagen gels. By focusing below the surface monolayer 48 h after initial seeding, control SK-LMS-1 cells were seen to invade the underlying collagen matrix mostly as single elongated cells (Figure 10). Invasion was almost totally inhibited by addition of the synthetic metalloproteinase inhibitor BB94 (1  $\mu$ g/ml), suggesting a requirement for metalloproteinase activity (data not shown). Qualitative observations revealed that 24 h after seeding, control vector and antisense TIMP-3 transfectants had already penetrated below the surface of the gel, whereas TIMP-3 overexpressors were still mostly confined to the gel surface. Forty-eight hours after seeding, the three cell lines had invaded the underlying gel to different extents; TIMP-3 overexpressors were the least invasive (Figure 10b), TIMP-3 antisense transfectants were most invasive (Figure 10c), while the vector-transfected control cells were between these two extremes (Figure 10a). A quantitative analysis of the number of cells which had

migrated to depths of 100  $\mu$ m and 200  $\mu$ m below the surface of the gel 48 h after seeding demonstrated that TIMP-3 overexpressors were less invasive than control cells, whereas TIMP-3 antisense transfectants were significantly more invasive ( $P < 0.001$ ; Figure 10d).

## Discussion

The TIMP family of metalloproteinase inhibitors regulate the activity of proteinases such as collagenases, gelatinases and stromelysins, and several lines of evidence suggest that TIMPs are required for extracellular matrix (ECM) homeostasis (reviewed in Stetler-Stevenson *et al.*, 1996; Anand-Apte *et al.*, 1996). TIMP-3 was originally purified from Rous sarcoma virus-infected chicken embryo fibroblasts (Blenis and Hawkes, 1984; Staskus *et al.*, 1991). Isolation of the TIMP-3 cDNA and recombinant expression revealed that the encoded protein promoted detachment of transformed cells from the ECM, accelerated morphological changes characteristic of transformation, and enhanced the growth of normal cells in low serum conditions (Pavloff *et al.*, 1992; Yang and Hawkes, 1992). TIMP-3 was also identified as a serum-inducible delayed early-response gene in human diploid fibroblasts (Wick *et al.*, 1994). At least two specific pathological ECM-related defects have been linked to TIMP-3: specific inherited mutations in the TIMP-3 gene cause night blindness in Sorsby's fundus dystrophy (Weber *et al.*, 1994), and elevated retinal TIMP-3 mRNA expression has been correlated with simplex retinitis pigmentosa (Jones *et al.*, 1994).

TIMP-3 is expressed in adult kidney, placenta, lung, ovary, uterus, brain, muscle, and bone (Leco *et al.*, 1994; Hurskainen *et al.*, 1996). TIMP-3 is also

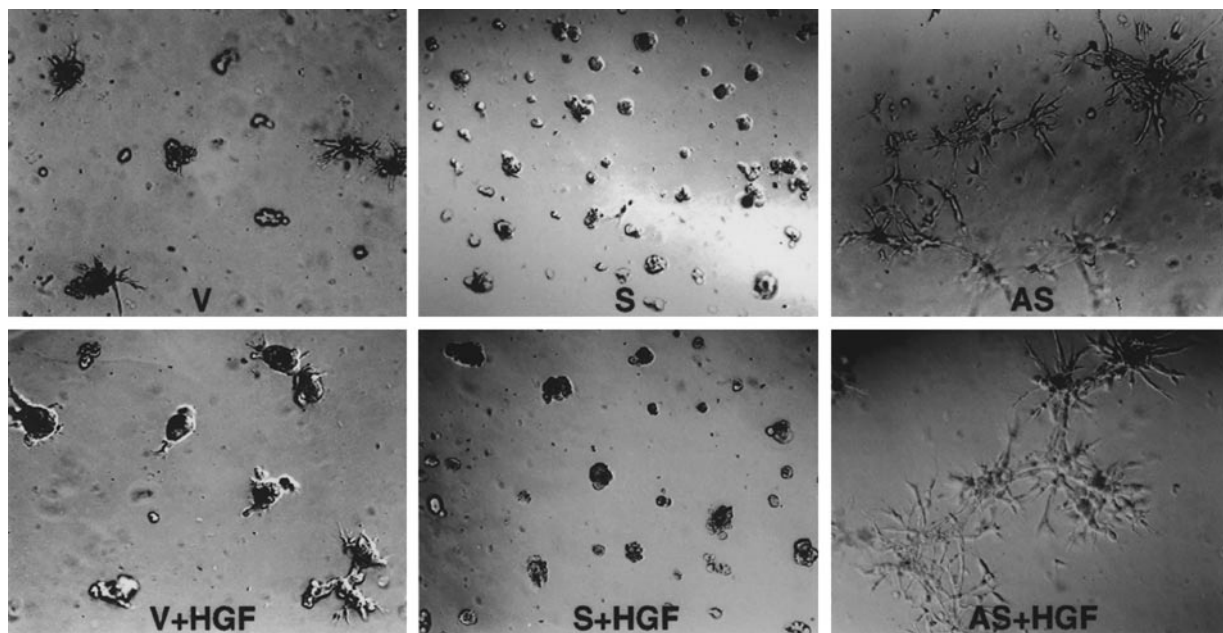


**Figure 9** Effects of TIMP-3 overexpression and antisense suppression on SK-LMS-1 cell invasion into Matrigel matrices. Cells seeded on three-dimensional Matrigel matrices in growth medium alone (upper panels) or growth medium supplemented with HGF (lower panels) were photographed 96 h later by focusing below the surface of the gel using phase contrast optics and a 20 $\times$  objective as described in Materials and methods. SK-LMS-1 cells transfected with vector alone (V, left panels) exhibited some short processes that extend into the matrix, which are not visible in cells transfected with full-length TIMP-3 sense cDNA (S, center panels), while cells transfected with antisense to TIMP-3 were highly branched and extended multiple processes into the underlying matrix (AS, right panels)

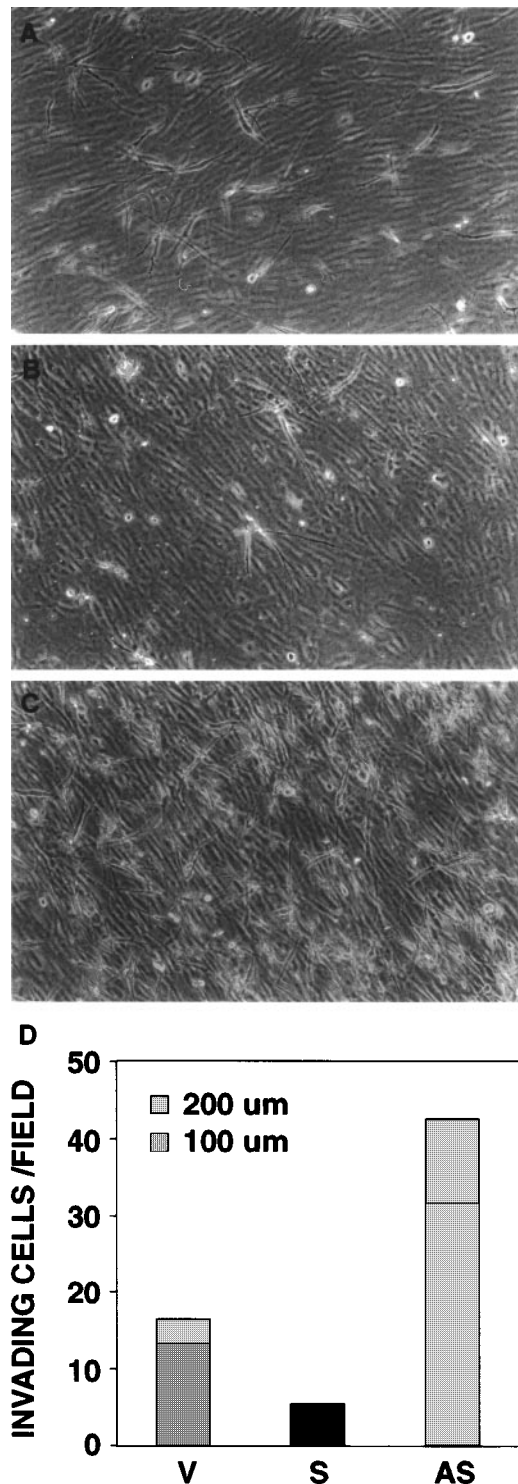


**Figure 10** Effects of TIMP-3 overexpression and antisense suppression on SK-LMS-1 cell invasion into collagen gels. Cells were seeded onto three-dimensional collagen gels and the cultures were photographed 48 h later by focusing below the surface of the gel. Cells which have migrated from the surface monolayer into the underlying collagen matrix can be appreciated. A small number of SK-LMS-1 transfected with full length TIMP-3 cDNA (b) have invaded the collagen gel when compared to cells transfected with control vector (a). In contrast, a large number of SK-LMS-1 cells transfected with full length antisense TIMP-3 cDNA have migrated into the collagen matrix (c). Cells were photographed at a magnification of  $60\times$ , final magnification is approximately  $45\times$ . Invasion was quantitated as described in Materials and methods by counting the number of cells which had migrated 100  $\mu\text{m}$  (dark shaded portion of the columns) or 200  $\mu\text{m}$  (light shaded portion of the columns) below the surface of the gel 48 h after seeding (d). In the case of SK-LMS-1 transfected with

expressed developmentally in the latter half of gestation primarily in cartilage, placental trophoblasts, various epithelia, and muscle (Apte *et al.*, 1994). Consistent with its high expression in kidney, we identified TIMP-3 by DD-PCR as an HGF-induced gene in MDCK cells. HGF-induction of TIMP-3 in keratinocytes and mammary epithelial cells suggests that it may be a general HGF response. The high level of TIMP-3 expression in placental trophoblasts is noteworthy in light of the role of HGF in directing placental development. Two independent HGF gene deletion studies reported severe placental defects, particularly in the number and organization of trophoblast cells (Schmidt *et al.*, 1995; Uehara *et al.*, 1995). The proliferation and differentiation of trophoblast cells, which are presumably derived from embryonic ectoderm, is normally stimulated by HGF produced by allantoic mesenchyme (Uehara *et al.*, 1995). The role of HGF as a paracrine mediator of epithelial morphogenesis in this system exemplifies what has become a well-accepted paradigm of HGF action: HGF secreted by mesenchymal cells stimulates its receptor expressed in adjacent epithelial cells in various tissues throughout normal development (Rubin *et al.*, 1991; Sonnenberg *et al.*, 1993). Although the role of TIMP-3 in trophoblast differentiation remains to be determined, HGF is likely to regulate its expression in this setting.

The extensive use of tissue culture model systems has helped uncover the mechanisms by which HGF exerts its pleiotropic effects. HGF stimulates scattering of MDCK cells (Stoker and Perryman, 1985), promotes their invasion through ECM substrates (Giordano *et al.*, 1993; Rong *et al.*, 1994), and induces tubular morphogenesis in collagen or fibrin gels (Montesano *et al.*, 1991). These processes are thought to depend, in part, upon ECM remodeling via controlled proteolytic degradation, associated with an HGF-induced increase in u-PA and its receptor (Montesano *et al.*, 1991; Pepper *et al.*, 1992). Two other members of the metalloproteinase family, stromelysin-1 (MMP-3) and collagenase-1 (MMP-1), are induced by HGF in primary keratinocytes, suggesting a general role for these enzymes in HGF-induced ECM remodeling (Dunsmore *et al.*, 1996). While HGF-stimulated production of u-PA, MMP-1, and MMP-3 led to their gradual accumulation over 24–48 h (Pepper *et al.*, 1992; Dunsmore *et al.*, 1996), we observed that HGF-stimulated TIMP-3 secretion was maximal within 6–8 h, and decreased thereafter. This is consistent with the cell-cycle specificity of TIMP-3 induction reported by Wick and coworkers (1994), where it was noted that no other known gene exhibited such G1-specific induction. These data, together with the absence of significant changes in the activities of MMP-2 and MMP-9 during this period reported here, suggest that ECM turnover is temporarily suspended, then gradually increases, following HGF stimulation.

full length TIMP-3 cDNA, no cell per random field was found 200  $\mu\text{m}$  below the surface monolayer. The total height of the columns represents the additive number of cells per field at the two focal planes examined. Results are shown as mean number of invading cells per photographic field. The s.e.m. was less than 10% of mean values;  $n=15$  fields;  $P<0.001$  by ANOVA single factor test



During the first 6 h of HGF treatment, MDCK cells spread (increasing projected surface area at least twofold), intercellular contacts remain intact, and the number and size of F-actin stress fibres increase, events that are thought to represent increased cell anchorage (Stoker and Perryman, 1985; Dowrick *et al.*, 1991; Ridley *et al.*, 1995). Cells at the colony periphery also show increased lamellipodia and membrane ruffling, and all of these early events appear to require Ras and Rac signaling (Ridley *et al.*, 1995). From 6–18 h, intercellular contacts diminish, stress fibers disappear, and cell motility increase (Stoker and Perryman, 1985; Dowrick *et al.*, 1991). Although the initial cell spreading coincides temporally with rising TIMP-3 secretion, two observations suggest that it may be TIMP-3 independent: (1) cycloheximide inhibited cell spreading only slightly, but potentially inhibited subsequent scattering (Ridley *et al.*, 1995), suggesting that spreading occurs in the absence of increased TIMP-3 protein synthesis; and (2) SK-LMS-1 cells overexpressing TIMP-3 actually show less projected cell surface area than vector controls (Figure 5). Interestingly, however, the morphology of SK-LMS-1/TIMP-3 antisense transfectants, and preliminary observations (not shown), suggest that TIMP-3 may somehow contribute to the increased cell adhesion that is believed to occur in this initial phase of MDCK cell response.

Several differences in morphology between SK-LMS-1/TIMP-3 sense and antisense transfectants correlate with HGF-stimulated changes in MDCK cells. The TIMP-3 overexpressing cells form more tightly grouped colonies than control or antisense transfectants, and intercellular contacts are maintained in the initial phase of HGF-stimulated MDCK cell scatter. The later disruption in MDCK intercellular contacts temporally overlaps peak and declining TIMP-3 levels, and coincides with the gradual shift toward ECM degradation that would accompany the long term HGF-induction of several MMPs. SK-LMS-1/TIMP-3 transfectants more closely resemble MDCK cells than controls, particularly the lack of isolated single cells, polygonal cell shape, and strict contact-inhibition of growth. Coincidentally, steady-state TIMP-3 expression by MDCK was found to be much greater than the normal fibroblasts or other epithelial cell types examined. At confluence, MDCK cells form a monolayer and do not overgrow (or migrate over) each other, even in the presence of HGF (Dowrick *et al.*, 1991). SK-LMS-1/TIMP-3 transfectants also exhibit more strict monolayer, contact-inhibited growth than control transfectants. This is in striking contrast to SK-LMS-1/TIMP-3 antisense transfectants: cells are spindle-shaped, lack tight intercellular contacts, lack contact inhibition, and grow at a faster rate than controls.

Although the mechanism by which TIMP-3 exerts such profound changes on cell morphology and growth is not known, evidence from studies of all TIMPs supports two distinct pathways. Intracellular signals generated in response to ECM turnover, such as those transduced by integrin receptors, may be modulated by TIMP-mediated suppression of MMP activity (Huhtala *et al.*, 1995). For example, MMP activity expressed by melanoma cells seeded on a collagen gel substrate changed the basis of the cell-ECM interaction from ligation of the  $\alpha_5\beta_1$ -integrin to an  $\alpha_1$ -mediated

interaction (Montgomery *et al.*, 1994). The second mechanism – the existence of specific cell surface TIMP receptors – has been proposed to explain the growth promoting activities of TIMP-1 and -2 in erythroid cells, fibroblasts, and keratinocytes (Docherty *et al.*, 1985; Golde *et al.*, 1980; Westbrook *et al.*, 1984; Avalos *et al.*, 1988; Stetler-Stevenson *et al.*, 1992; Bertaux *et al.*, 1990). The existence of two pathways may hold an explanation for the apparent disparity between the data presented here – decreased proliferation by TIMP-3 overexpressors and enhanced proliferation by antisense TIMP-3 transfectants – and reports of growth promotion by TIMP-1 and -2.

We observed that TIMP-3 antisense suppression enhanced colony formation by SK-LMS-1 in soft agar, as well as their ability to invade three-dimensional Matrigel or collagen-I matrices, while TIMP-3 overexpression strongly inhibited both anchorage-independent growth and matrix invasion. These properties of TIMP-3 are consistent with those reported previously for TIMP-1 and -2. TIMP-1 lowers the metastatic potential of melanoma cells (Khokha, 1994), TIMP-1 suppression confers oncogenicity to normal fibroblasts (Khokha *et al.*, 1989), and TIMP-1 gene deletion results in enhanced invasion of normal differentiated cells and altered metastasis of transformed cells (Alexander and Werb, 1992; Soloway *et al.*, 1996). Moreover, down-regulation of TIMP-1 and -2 may contribute significantly to the invasive potential of human glioblastoma (Mohanam *et al.*, 1995), and we have observed that several tumor cell lines, particularly those derived from metastatic tumors, express little or no TIMP-3 protein. Many other studies document the positive role of MMPs in promoting tumor invasion and metastasis (reviewed in Stetler-Stevenson *et al.*, 1996). Thus TIMP/MMP imbalance, caused by TIMP suppression or MMP overexpression, can result in increased cellular invasiveness. The modulation of this balance appears to be an important and highly orchestrated cellular response to HGF: an early phase of TIMP-3 induction leading to MMP suppression, followed by a later phase of MMP induction and increased cell invasiveness. HGF does not appear to modulate TIMP-1 expression in the cell lines used in our study (data not shown), and extensive analysis of TIMP-2 expression suggests that it is largely constitutive (Leco *et al.*, 1994). Together with the results reported here, these findings support a pivotal role for TIMP-3 as an early mediator of HGF-regulated TIMP/MMP balance.

HGF/c-Met signaling plays an essential role in normal development and adult homeostasis at least in part by mediating mesenchymal-to-epithelial conversion and promoting epithelial organization and differentiation. The inappropriate expression of c-Met in certain mesenchymal cells can lead to a carcinogenic transformation in which the tumor cells express both mesenchymal and epithelial markers (Tsarfaty *et al.*, 1994). We have found that HGF induces the transient expression of TIMP-3, and that this protein can suppress anchorage-independent cell growth. Since HGF also induces the sustained production of MMPs that promote cellular invasion, the observed sequence of TIMP and MMP induction events in the appropriate milieu may be essential for normal HGF-directed development. Inappropriate sustained HGF

signaling, such as that observed in a variety of tumors that coexpress c-Met and HGF, would be expected to result in a long term reduction in TIMP-3 expression and sustained MMP accumulation. The resulting TIMP/MMP imbalance may contribute to a highly invasive and possibly metastatic phenotype.

## Materials and methods

### Materials

Tissue culture medium, growth supplements, and RT-H<sup>-</sup> were obtained from GIBCO-BRL. Plasticware was obtained from Costar and Nunc. Human recombinant HGF and recombinant TGF- $\beta$  were gifts from Drs George Vande Woude and Anita Roberts, respectively. Purified chicken TIMP-3 protein standard was generously provided by Dr Susan Hawkes. Two polyclonal TIMP-3 antibodies raised against its C-terminal amino acid sequence, and cross-reactive with human, mouse, and chicken TIMP-3, were used; one was obtained from Triple Point Biologics, and the other was a gift from Dr Susan Hawkes. Affinity-purified anti-gelatinase-A and -B antibodies were gifts from Dr William Stetler-Stevenson. Purified MMP-2 (72 kDa) was from Boehringer Mannheim. Recombinant human EGF was obtained from Collaborative Research. Recombinant human PDGF, IGF-1 and bFGF were from Upstate Biotechnology, Inc. Recombinant human KGF was prepared as described previously (Ron *et al.*, 1993). Recombinant NK2 was prepared as described previously (Stahl *et al.*, 1997). RNazolB was obtained from Tel-Test. Nytran membrane was obtained from S&S. p-Iodotetrazolium violet and gelatin-agarose were from Sigma. T7 polymerase was obtained from Pharmacia. [<sup>32</sup>P]dCTP was from Amersham. Reagents for DD-PCR were obtained from Gen Hunter, Inc. The TA cloning vector was obtained from Invitrogen. Matrigel was purchased from Collaborative Research/Becton Dickinson. Synthetic metalloproteinase inhibitor BB94 was the generous gift of Drs J Gordon and P Brown, British Biotechnology, Cowley, UK.

### Tissue culture and cell transfection

MDCK cells were grown at 37°C in DMEM supplement with 10% fetal bovine serum (FBS). Cells were grown in dishes that had been precoated with human fibronectin at 1  $\mu$ g/cm<sup>2</sup>. When the cells reached 60% confluency, the medium was replaced with DMEM + 5% FBS alone or with the indicated growth factors. The leiomyosarcoma cell line SK-LMS-1 was grown in DMEM + 10% FBS. NIH3T3 mouse fibroblasts were grown in DMEM + 10% calf serum. Full-length TIMP-3 cDNA in pCEV29 (Lorenzi *et al.*, 1996) in the sense or antisense orientation was transfected into SK-LMS-1 cells by calcium phosphate precipitation and stable transfectants were obtained by selection in media containing G418 (500  $\mu$ g/ml).

### RNA isolation and Northern blot analysis

MDCK cells were washed three times with ice-cold PBS and total RNA was isolated using RNazolB according to the manufacturer's protocol. RNA concentration was estimated by measuring absorbance at 260 nm. Samples of total RNA (15  $\mu$ g) were run on a 1% agarose/formaldehyde gel and transferred by capillary blotting onto Nytran membrane. Radioactive DNA probes were prepared using T7 polymerase and [<sup>32</sup>P]dCTP according to the manufacturer's instructions. Hybridization was performed in 50% formamide (40% for MDCK) followed by two high stringency washes at 58°C in 0.1  $\times$  SSC (0.2  $\times$  SSC for MDCK) and 0.1% SDS.

### Differential display

Total RNA (200 ng) isolated from MDCK cells grown in 5% serum alone or supplemented with HGF (50 ng/ml), or NK2 (300 ng/ml) was reverse transcribed with 200 U RT-H<sup>-</sup> with a one base anchored oligo dT primer. PCR reactions and subsequent product purifications were performed using the Gen Hunter Kit according to manufacturer's instructions. Final products were then subcloned using the TA cloning vector and subjected to restriction analysis and dideoxy sequencing.

### Immunoblotting

Subconfluent cell cultures were treated with HGF, or left untreated, for the time intervals indicated, and cell lysates were prepared by extraction on ice with 50 mM Tris buffer (pH 7.4) containing 1% Triton X-100, 0.1% SDS, and protease and phosphatase inhibitors. After clearing by high speed centrifugation, protein amount was determined using the BCA protein assay (Pierce). Equal amounts of protein were prepared in SDS sample buffer and samples were resolved by SDS-PAGE, transferred to PVDF, probed with anti-TIMP-3 and detected by chemiluminescence. A purified TIMP-3 standard was included in addition to conventional molecular mass standards.

### Cell growth rate, anchorage-independent growth, and photo-microscopy

The effects of TIMP-3 on SK-LMS-1 cell growth were quantitated by seeding multiwell tissue culture plates with SK-LMS-1 cells transfected with vector alone, full-length TIMP-3 cDNA, or full-length antisense TIMP-3 cDNA at a density of 100 cells/well. At various times, cells were fixed, stained with Giemsa, and multiple wells were scanned using a UMAX PowerLook II high resolution scanner. Quantitative densitometry and descriptive statistical analysis was performed on the stored images using NIH Image software. Mean values of optical density, in arbitrary units, were plotted on the Y-axis against days after seeding on the X-axis. The results of a representative experiment are shown.

Anchorage-independent growth in soft agar was performed and quantitated as described previously (DiFiore *et al.*, 1987). Briefly, SK-LMS-1 transfectants were suspended at tenfold serial dilutions ( $1 \times 10^5$  to  $1 \times 10^3$  cells) in 0.5% Seaplaque agarose in growth medium in duplicate. Cells were fed once a week with growth medium containing 10% FCS. Parallel sets of SK-LMS-1 transfectants were plated in duplicate into 60 mm dishes to determine the number of colonies formed per plating density. Cell colonies in the soft agar assays were visualized after staining with p-iodotetrazolium violet by brightfield microscopy using a Zeiss Axiovert 135TV microscope with a 2.5 $\times$  objective; general cell morphology was visualized by phase contrast microscopy with a 10 $\times$  objective. Percentage of soft agar growth was determined by counting the number of cells forming colonies of diameter greater than 50  $\mu$ m per total colony number. The percentage presented is the average of three measurements. Note that in antisense transfectants many cell colonies of diameter greater than 100  $\mu$ m were visualized. Digital images were recorded using a Hamamatsu XC77 CCD video camera, Hamamatsu Camera Controller Model C2400, IPLab Spectrum software (Signal Analytics, Inc.) and a Power Macintosh 7200 computer.

### Zymography

MDCK or SK-LMS-1 cells were washed in serum-free medium and incubated in the presence or absence of HGF for time intervals up to 18 h, as indicated in the figure

legends. Media were then collected and incubated at 4°C for 1 h with 100 µl gelatin-agarose equilibrated in 50 mM Tris-HCl, 150 mM NaCl, 5 mM CaCl<sub>2</sub>, and 0.02% Tween 20, pH 7.6 (Mazzieri *et al.*, 1997). The beads were washed three times with the equilibration buffer containing 200 mM NaCl, and proteins were extracted with 70 µl of non-reducing Laemmli buffer for SDS-PAGE. Equal volume of samples were loaded on Novex precast 10% gels for gelatin zymography according to the manufacturer's protocol to analyse gelatinase activity. Equal volumes of samples were analysed under reducing conditions by immunoblotting to determine the amount of each gelatinase, and equal loading of lanes was confirmed by staining parallel blots with Auro Dye Forte (Amersham). MDCK cell lysates were prepared by extraction on ice with 50 mM Tris buffer (pH 7.4) containing 0.5% Triton X-100, 150 mM NaCl, and protease and phosphatase inhibitors. Protein amount was determined by BCA protein assay (Pierce) and equal amounts of samples were analysed by immunoblotting to verify TIMP-3 induction.

#### In vitro invasion assays

A 50% solution of Matrigel in DMEM (300 µl) was added to each well of 48-well plates and kept at 37°C for 30 min to gel. SK-LMS-1/TIMP-3 transfectants, at a density of 25 000 cells/ml of DMEM + 5% FCS alone or supplemented with HGF, were seeded at 300 µl per well into the Matrigel-containing plates. Media were replaced and HGF was added every other day at 200 ng/ml. After 4 days cell invasion was photographed by focusing through the gel using phase contrast optics in a Zeiss Axiovert 135TV microscope with a 20× objective.

The invasion of cells into three-dimensional collagen gels was analysed essentially as described (Montesano and Orci, 1985). Briefly, eight volumes of a solution of type I collagen extracted from rat tail tendons (approximately 1.5 mg/ml) were quickly mixed with one volume of 10× MEM and one volume of sodium bicarbonate (11.76 mg/ml) on ice, and 400 µl aliquots of this mixture were dispensed into 16 mm tissue culture wells and allowed to gel at 37°C for 10 min. SK-LMS-1/TIMP-3 transfectants were seeded onto the gels at 2 × 10<sup>4</sup> cells/well in 400 µl of complete medium. After 48 h, the cultures were fixed *in situ* with 2.5% glutaraldehyde in 100 mM sodium cacodylate buffer (pH 7.4). To quantitate invasion, in each of three separate experiments, five randomly selected fields measuring 1 × 1.4 mm were photographed at two different levels (100 µm and 200 µm) beneath the surface monolayer using the calibrated fine focusing micrometer and the 10× phase contrast objective of a Nikon Diaphot TMD inverted photomicroscope. Invasion was quantitated on positive prints by counting the number of cells identifiable in each photographic field. Values are shown as mean number of invading cells per photographic field, and statistical significance was determined using the ANOVA single factor test.

#### Acknowledgements

We thank Bill Taylor, Veena Kapoor, Diane Breckenridge and Juddi Yeh for technical assistance, and Marcio Chedid, Matt Lorenzi and Jeff Rubin for helpful advice. This work was supported in part (RM and JVS) by a grant from the Swiss National Science Foundation (No. 31-43364.95).

#### References

- Albini A, Iwamoto Y, Kleinman HK, Martin GR, Aaronson SA, Kozlowski JM and McEwan RN. (1987). *Cancer Res.*, **47**, 3239–3245.
- Alexander CM and Werb Z. (1992). *J. Cell Biol.*, **118**, 727–739.
- Anand-Apte B, Bao L, Smith R, Iwata K, Olsen BR, Zetter B and Apte SS. (1996). *Biochem. Cell Biol.*, **74**, 853–862.
- Apte SS, Mattei MG and Olsen BR. (1994). *Genomics*, **19**, 86–90.
- Apte SS, Olsen BR and Murphy G. (1995). *J. Biol. Chem.*, **270**, 14313–14318.
- Avalos BR, Kaufman SE, Tomonaga M, Williams RE, Golde DW and Gasson JC. (1988). *Blood*, **71**, 1721–1725.
- Bardelli A, Maina F, Gout I, Fry MJ, Waterfield MD, Comoglio PM and Ponzetto C. (1992). *Oncogene*, **7**, 1973–1978.
- Bertaux B, Hornebeck W, Courtalon A, Lebreton C and Dubertret L. (1990). *Pathol. Biol.*, **38**, 1029–1033.
- Bian J, Wang Y, Smith MR, Kim H, Jacobs C, Jackman J, Kung HF, Colburn NH and Sun Y. (1996). *Carcinogenesis*, **17**, 1805–1811.
- Blenis J and Hawkes SP. (1984). *J. Biol. Chem.*, **259**, 11563–11570.
- Boccaccio C, Gaudino G, Gambarotta G, Galimi F and Comoglio PM. (1994). *J. Biol. Chem.*, **269**, 12846–12851.
- Bottaro DP, Rubin JS, Faletto DL, Chan AM, Kmiecik TE, Vande Woude GF and Aaronson SA. (1991). *Science*, **251**, 802–804.
- Chan AM, Rubin JS, Bottaro DP, Hirschfield DW, Chedid M and Aaronson SA. (1991). *Science*, **254**, 1382–1385.
- Cioce V, Csaky KG, Chan AM, Bottaro DP, Taylor WG, Jensen R, Aaronson SA and Rubin JS. (1996). *J. Biol. Chem.*, **271**, 13110–13115.
- Di Fiore PP, Pierce JH, Fleming TP, Hazan R, Ullrich A, King CR, Schlessinger J and Aaronson SA. (1987). *Cell*, **51**, 1063–1070.
- Docherty AJP, Lyons A, Smith BJ, Wright EM, Stephens PE, Harris TJR, Murphy G and Reynolds JJ. (1985). *Nature*, **318**, 66–69.
- Dowrick PG, Prescott AR and Warn RM. (1991). *Cytokine*, **3**, 299–310.
- Dunsmore SE, Rubin JS, Kivacs SO, Chedid M, Parks WC and Welgus HG. (1996). *J. Biol. Chem.*, **271**, 24576–24582.
- Fafeur V, Tulasne D, Queva C, Vercamer C, Dimster V, Mattot V, Stehelin D, Desbiens X and Vendenbunder B. (1997). *Cell Growth & Diff.*, **8**, 655–665.
- Fixman ED, Naujokas MA, Rodrigues GA, Moran MF and Park M. (1995). *Oncogene*, **10**, 237–249.
- Fournier TM, Kamikura D, Teng K and Park M. (1996). *J. Biol. Chem.*, **271**, 22211–22217.
- Giordano S, Zhen Z, Medico E, Gaudino G, Galimi F and Comoglio PM. (1993). *Proc. Natl. Acad. Sci. USA*, **90**, 649–653.
- Gohda E, Matsunaga T, Kataoka H, Takebe T and Yamamoto I. (1994). *Cytokine*, **6**, 633–640.
- Golde DW, Bersch N, Quan SG and Lusis AJ. (1980). *Proc. Natl. Acad. Sci. USA*, **77**, 593–596.
- Graziani A, Gramaglia D, Cantley LC and Comoglio PM. (1991). *J. Biol. Chem.*, **266**, 22087–22090.
- Huhtala P, Humphries MJ, McCarthy JB, Tremble PM, Werb Z and Damsky CH. (1995). *J. Cell Biol.*, **26**, 16011–16014.
- Hurskainen T, Hoyhtya M, Tuuttila A, Oikarinen A and Autio-Harmainen H. (1996). *J. Histochem. Cytochem.*, **12**, 1379–1388.

- Jeffers M, Rong S and Vande Woude GF. (1996). *Mol. Cell. Biol.*, **16**, 1115–1125.
- Jones SE, Jomary C and Neal MJ. (1994). *FEBS Lett.*, **352**, 171–174.
- Khokha R. (1994). *J. Natl. Cancer Inst.*, **86**, 299–304.
- Khokha R, Waterhouse P, Yagel S, Lala PK, Overall CM, Norton G and Denhardt DT. (1989). *Science*, **243**, 947–950.
- Leco KJ, Khokha R, Pavloff N, Hawkes SP and Edwards DR. (1994). *J. Biol. Chem.*, **269**, 9352–9360.
- Longati P, Bardelli A, Ponzetto A, Naldini L and Comoglio PM. (1994). *Oncogene*, **9**, 49–57.
- Lorenzi MV, Horii Y, Yamanaka R, Sakaguchi K and Miki T. (1996). *Proc. Natl. Acad. Sci. USA*, **93**, 8956–8961.
- Matsumoto K, Okazaki H and Nakamura T. (1992). *Biochem. Biophys. Res. Commun.*, **188**, 235–243.
- Mazzieri R, Masiero L, Zanetta L, Monea S, Onisto M, Garbisa S and Mignatti P. (1997). *EMBO J.*, **16**, 2319–2332.
- Michalopoulos GK and DeFrances MC. (1997). *Science*, **276**, 60–66.
- Mohanam S, Wang SW, Rayford A, Yamamoto M, Sawaya R, Nakajima M, Liotta LA, Nicolson GL, Stetler-Stevenson WG and Rao JS. (1995). *Clin. Exp. Metastasis*, **13**, 57–62.
- Montesano R and Orci L. (1985). *Cell*, **42**, 469–477.
- Montesano R, Matsumoto K, Nakamura T and Orci L. (1991). *Cell*, **67**, 901–908.
- Montgomery AM, Reisfeld RA and Cheresch DA. (1994). *Proc. Natl. Acad. Sci. USA*, **91**, 8856–8860.
- Naldini L, Vigna E, Ferracini R, Longati P, Gaudino L, Prat M and Comoglio PM. (1991a). *Mol. Cell. Biol.*, **11**, 1793–1803.
- Naldini L, Vigna E, Narsimhan RP, Gaudino G, Zarnegar R, Michalopoulos GA and Comoglio PM. (1991b). *Oncogene*, **6**, 501–504.
- Nusrat A, Parkos CA, Bacarra AE, Godowski PJ, Delp-Archer C, Rosen EM and Madara JM. (1994). *J. Clin. Invest.*, **93**, 2056–2065.
- Park M, Dean M, Kaul K, Braun MJ, Gonda MA and Vande Woude G. (1987). *Proc. Natl. Acad. Sci. USA*, **84**, 6379–6383.
- Pavloff N, Staskus PW, Kishnani NS and Hawkes SP. (1992). *J. Biol. Chem.*, **267**, 17321–17326.
- Pellicci G, Giordano S, Zhen Z, Salcini AE, Lanfrancone L, Bardelli A, Panayotou G, Waterfield MD, Ponzetto C, Pellicci PG and Comoglio. (1995). *Oncogene*, **10**, 1631–1638.
- Pepper MS, Matsumoto K, Nakamura T, Orci L and Montesano R. (1992). *J. Biol. Chem.*, **267**, 20493–20496.
- Ponzetto C, Bardelli A, Zhen Z, Maina F, della Zonca P, Giordano S, Graziani A, Gramaglia D, Cantley LC and Comoglio PM. (1991). *J. Biol. Chem.*, **266**, 22087–22090.
- Ponzetto C, Bardelli A, Zhen Z, Maina F, della Zonca P, Giordano S, Graziani A, Panayotou G and Comoglio PM. (1994). *Cell*, **77**, 261–271.
- Rahimi N, Tremblay E and Elliot B. (1996). *J. Biol. Chem.*, **271**, 24850–24855.
- Ridley AJ, Comoglio PM and Hall A. (1995). *Mol. Cell. Biol.*, **15**, 1110–1122.
- Ron D, Bottaro DP, Finch P, Morris D, Rubin J and Aaronson SA. (1993). *J. Biol. Chem.*, **268**, 2984–2988.
- Rong S, Segal S, Anver M, Resau JH and Vande Woude GF. (1994). *Proc. Natl. Acad. Sci. USA*, **91**, 4731–4735.
- Royal I and Park M. (1995). *J. Biol. Chem.*, **270**, 27780–27787.
- Rubin JS, Bottaro DP and Aaronson SA. (1993). *Biochim. Biophys. Acta*, **1155**, 357–371.
- Rubin JS, Chan AM, Bottaro DP, Burgess WH, Taylor WG, Cech AC, Hirschfield DW, Wong J, Miki T, Finch PW and Aaronson SA. (1991). *Proc. Natl. Acad. Sci. USA*, **88**, 415–419.
- Sakurai H and Nigam SK. (1997). *Am. J. Physiol.*, **272**, 139–146.
- Savagner P, Yamada KM and Thiery JP. (1997). *J. Cell Biol.*, **137**, 1403–1419.
- Schmidt C, Bladt F, Goedecke S, Brinkmann V, Zschiesche W, Sharpe M, Gherardi E and Birchmeier C. (1995). *Nature*, **373**, 699–702.
- Soloway PD, Alexander CM, Werb Z and Jaenisch R. (1996). *Oncogene*, **13**, 2307–2314.
- Sonnenberg E, Meyer D, Weidner KM and Birchmeier C. (1993). *J. Cell Biol.*, **123**, 223–235.
- Sponsel HT, Breckon R, Hammond W and Anderson RJ. (1994). *Am. J. Physiol.*, **267**: F257–F264.
- Stahl SJ, Wingfield PT, Kaufman JD, Pannell LK, Cioce V, Sakata H, Taylor WG, Rubin JS and Bottaro DP. (1997). *Biochem. J.*, **326**, 763–772.
- Staskus PW, Masiarz FR, Pallanck LJ and Hawkes SP. (1991). *J. Biol. Chem.*, **266**, 449–454.
- Stetler-Stevenson WG, Bersch N and Golde DW. (1992). *FEBS Lett.*, **296**, 231–234.
- Stetler-Stevenson WG, Hewitt R and Corcoran M. (1996). *Semin. Cancer Biol.*, **3**, 147–154.
- Stoker M and Perryman M. (1985). *J. Cell Sci.*, **77**, 209–223.
- Tsarfaty I, Rong S, Reseau JH, Rulong S, Da Silva PP and Vande Woude GF. (1994). *Science*, **263**, 98–101.
- Uehara Y, Minowa O, Mori C, Shiota K, Kuno J, Noda T and Kitamura N. (1995). *Nature*, **373**, 702–705.
- Watanabe S, Hirose M, Wang XE, Maehiro K, Murai T, Kobayashi O, Nagahara A and Sato N. (1994). *Biochem. Biophys. Res. Commun.*, **199**, 1453–1460.
- Weber BHF, Vogt G, Pruett RC, Stohr H and Felbor U. (1994). *Nature Genet.*, **8**, 352–355.
- Weidner KM, Behrens J, Vanderkerckhove J and Birchmeier W. (1990). *J. Cell Biol.*, **111**, 2097–2108.
- Weidner MK, Di Cesare S, Sachs M, Brinkmann V, Behrens J and Birchmeier W. (1996). *Nature*, **384**, 173–176.
- Weidner MK, Sachs M and Birchmeier W. (1993). *J. Cell Biol.*, **121**, 145–154.
- Westbrook CA, Gasson JC, Gerber SE, Selsted ME and Golde DW. (1984). *J. Biol. Chem.*, **259**, 9992–9996.
- Wick M, Burger C, Brusselbach S, Lucibello FC and Muller R. (1994). *J. Biol. Chem.*, **269**, 18953–18960.
- Wojta J, Nakamura T, Fabry A, Hufnagel P, Beckmann R, McGrath K and Binder BR. (1994). *Blood*, **84**, 151–157.
- Yang TT and Hawkes SP. (1992). *Proc. Natl. Acad. Sci. USA*, **89**, 10676–10680.
- Zarnegar R and Michalopoulos GK. (1995). *J. Cell Biol.*, **129**, 1177–1180.
- Zhu H, Naujokas MA, Fixman ED, Torossian K and Park M. (1994). *J. Biol. Chem.*, **269**, 29943–29948.